HEALTH AND MEDICINE

Ceftazidime-avibactam has potent sterilizing activity against highly drug-resistant tuberculosis

Devyani Deshpande,[1] Shashikant Srivastava,[1] Moti Chapagain,[1] Gesham Magombedze,[1] Katherine R. Martin,[1] Kayle N. Cirrincione,[1] Pooi S. Lee,[1] Thearith Koeuth,[1] Keertan Dheda,[2] Tawanda Gumbo[1,2]*

There are currently many patients with multidrug-resistant and extensively drug-resistant tuberculosis. Ongoing transmission of the highly drug-resistant strains and high mortality despite treatment remain problematic. The current strategy of drug discovery and development takes up to a decade to bring a new drug to clinical use. We embarked on a strategy to screen all antibiotics in current use and examined them for use in tuberculosis. We found that ceftazidime-avibactam, which is already used in the clinic for multidrug-resistant Gram-negative bacillary infections, markedly killed rapidly growing, intracellular, and semidormant *Mycobacterium tuberculosis* in the hollow fiber system model. Moreover, multidrug-resistant and extensively drug-resistant clinical isolates demonstrated good ceftazidime-avibactam susceptibility profiles and were inhibited by clinically achievable concentrations. Resistance arose because of mutations in the transpeptidase domain of the penicillin-binding protein PonA1, suggesting that the drug kills *M. tuberculosis* bacilli via interference with cell wall remodeling. We identified concentrations (exposure targets) for optimal effect in tuberculosis, which we used with susceptibility results in computer-aided clinical trial simulations to identify doses for immediate clinical use as salvage therapy for adults and young children. Moreover, this work provides a roadmap for efficient and timely evaluation of antibiotics and optimization of clinically relevant dosing regimens.

INTRODUCTION

Highly drug-resistant tuberculosis (TB) has left a large number of patients therapeutically destitute and functionally incurable (*1*, *2*). In South Africa, we found that 60% of such difficult-to-treat patients have unfavorable outcomes and are dead within 10 months of discharge (*3*). These highly drug-resistant cases spread the infection before death, and 50% of the secondary cases were dead by the end of the study. Newer antibiotics such as bedaquiline and delamanid improve outcomes but do not eliminate treatment failure. In patients with extensively drug-resistant TB receiving bedaquiline, the 24-month treatment failure rate was 38%, and patients with isolates resistant to both bedaquiline and delamanid are being documented with increasing frequency (*4*–*6*). The field urgently needs new treatments that can be deployed immediately without waiting for drug and clinical development programs that can take almost a decade.

One solution is reuse of antibiotics and other therapies with proven clinical safety records that are already known to penetrate lung lesions. We disregarded the standard dogma that only certain special antibiotic classes would be effective against *Mycobacterium tuberculosis* (*Mtb*) and created a program to deliberately examine all antibacterial agents in current clinical use.

We screened several antibiotic compounds in test tubes and then quickly moved to identify optimal doses for possible clinical use on the basis of the hollow fiber system model of TB (HFS-TB) (*7*). The HFS-TB allows for quick examination of drug efficacy based on human lung pharmacokinetics and for immediate translation of results from the laboratory to the clinic. The HFS-TB has a 94% predictive accuracy for clinical therapeutic events, such as dose, concentrations/exposures optimal in patients, and expected rates of clinical efficacy, and has been formally qualified as a drug development tool by the European Medicines Agency (EMA) and endorsed by the U.S. Food and Drug Administration (FDA) for this purpose (*8*–*10*).

Recent chemical screens have shown several older cephalosporins, in combination with the β-lactamase inhibitor clavulanate, as potential anti-TB agents (*11*). However, there are several drawbacks. First, clavulanate inhibition of *Mtb*'s broad-spectrum β-lactamase, BlaC, is slow and relatively inefficient. Second, clavulanate is currently only available for immediate use in combination with amoxicillin and not with cephalosporins. Third, amoxicillin-clavulanate administered for several months for TB is likely to be associated with high rates of side effects, such as diarrhea. We screened several other cephalosporins for anti-TB effect when in combination with the non–β-lactam β-lactamase inhibitor avibactam, which potently inhibits BlaC. One of these, ceftazidime, was first marketed almost 40 years ago and has no activity against *Mtb* and other Gram-positive bacteria (*12*). It was recently coformulated with avibactam, and this combination is already in clinical use for Gram-negative bacterial infections. Ceftazidime-avibactam (CAV) has a serum to lung epithelial lining fluid penetration of 32%, which makes it a good drug for pneumonias (*13*). We tested for CAV efficacy in the HFS-TB using clinically achievable intrapulmonary pharmacokinetics. We examined three *Mtb* metabolic subpopulations encountered in cavitary TB: logarithmic phase growth bacteria (log-phase growth) that are ordinarily killed by isoniazid in what is defined as bactericidal activity, intracellular *Mtb*, and semidormant bacteria under acidic conditions that are ordinarily killed by the combination of pyrazinamide and rifampin as part of the sterilizing effect (*14*–*17*). Other more potent cephalosporin-avibactam combinations were identified. However, we focused on CAV because this coformulation is available for immediate use as salvage therapy.

RESULTS

Program for rapid discovery and translation for antibiotic reuse to treat drug-resistant TB

Our screening, discovery, and translation program has several steps outlined in Fig. 1. In step 1, we screened for CAV activity against log-phase growth and intracellular *Mtb* and then identified the minimum inhibitory

[1]Center for Infectious Diseases Research and Experimental Therapeutics, Baylor Research Institute, Baylor University Medical Center, Dallas, TX 75204, USA. [2]Lung Infection and Immunity Unit, Division of Pulmonology and University of Cape Town (UCT) Lung Institute, Department of Medicine, UCT, Observatory, 7925, Cape Town, South Africa.
*Corresponding author. Email: tawanda.gumbo@BSWHealth.org
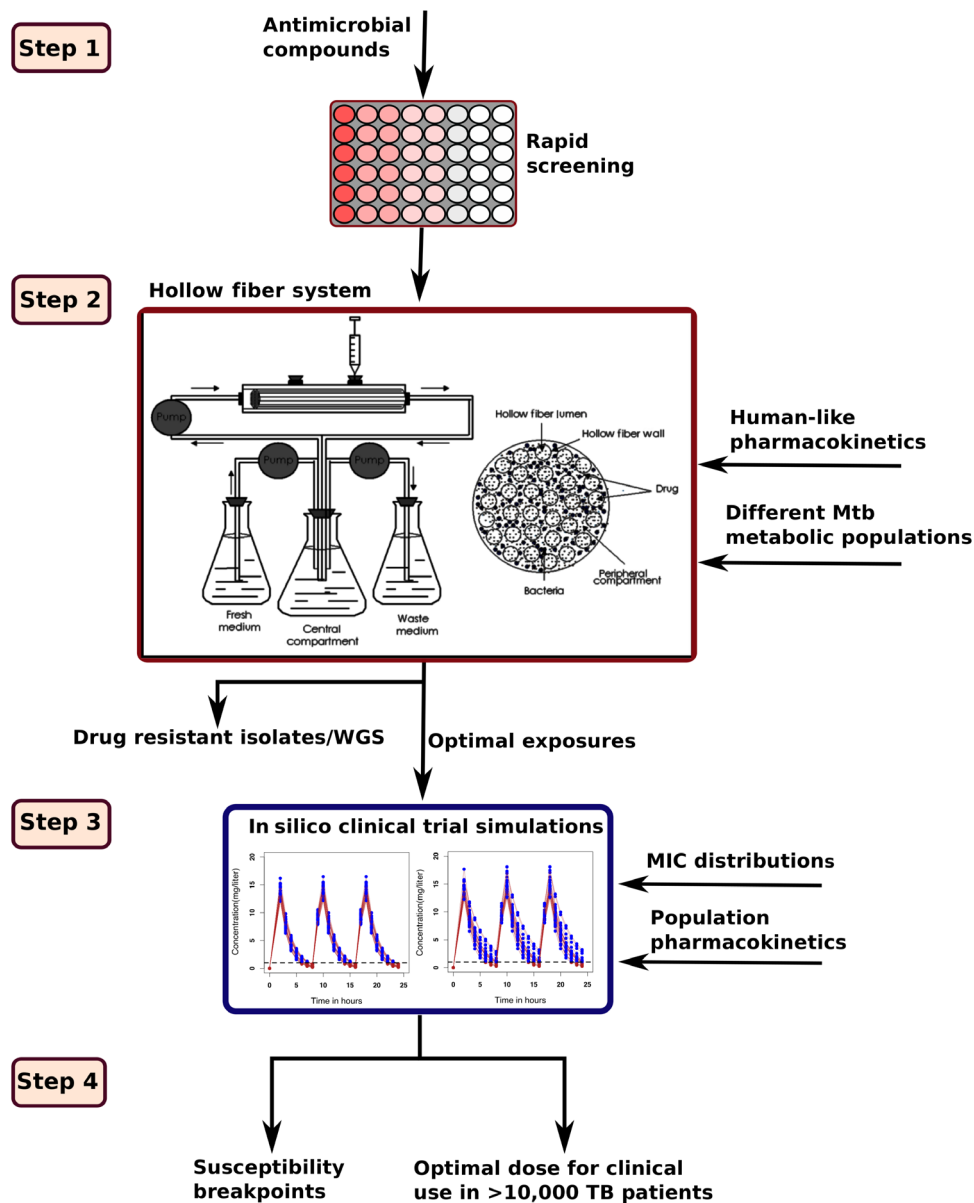
Fig. 1. Program for rapid screening and translation for reuse of antibiotics in TB. In the first step of the program, we examined the effect of CAV in comparison to standard first-line agents in intracellular and extracellular assays in a biosafety level 2 (BSL2) laboratory using avirulent *Mtb*. After demonstrating potential effectiveness, we then identified the MIC distribution in X/MDR-TB clinical strains from South Africa, in a BSL3 laboratory. In this first step, static concentrations of CAV were used. In step 2, we examined the efficacy of intrapulmonary concentration-time profiles of the CAV in the HFS-TB in several strains, for both bactericidal and sterilizing effect. These studies with dynamic concentrations of CAV against different *Mtb* metabolic subpopulations identified the concentrations and exposures associated with optimal kill and resistance suppression. They also generated CAV-resistant isolates, which then underwent whole-genome sequencing (WGS) to explore for mechanisms of effect. Step 3 takes place in silico, and uses output of step 2 as well as population-level pharmacokinetic parameters and measures of between-patient pharmacokinetic variability, plus MIC distributions from step 1, in Monte Carlo experiments to identify optimal clinical doses for use in patients with drug-resistant TB and for susceptibility breakpoints for decision-making of whom should be treated with the drug. Step 4 involves handing over of the clinical dose for immediate clinical trial studies and salvage therapy.

concentration (MIC) distribution in multidrug-resistant (MDR) and extensively drug-resistant (XDR) TB clinical isolates. In step 2, we used the CAV concentration-time profiles encountered in patients to identify the bactericidal and sterilizing effect rates in the HFS-TB. In step 3, the HFS-TB results were used together with the known between-patient pharmacokinetic variability of CAV to translate results to TB programs and for clinical trials. These steps allowed for delivery of a dosing regimen for clinical use in less than 9 months, making the drug immediately available for clinical studies.

Screening to identify effect of CAV against *Mtb*

The efficacy of first-line drugs in the HFS-TB, as well as in the clinic, is well known, which makes them ideal benchmarks. Figure 1 shows that our first step was to perform concentration-effect studies of the first-line drugs along with CAV against log-phase growth *Mtb* in Middlebrook 7H9 broth (hereinafter "broth") in test tubes and in phorbol myristate ester–activated human-derived THP-1 monocytes infected with *Mtb* in 24-well plates, using *Mtb* H37Ra, as described previously

(18–20). We used commercially available CAV (ceftazidime/avibactam ratio of 4:1), which was purchased from our hospital pharmacy. Maximal *Mtb* kill, denoted by the symbol E_{max}, was 0 to 1.43 $\log_{10}$ colony-forming units (CFU)/ml for pyrazinamide and 3.32 to 3.56 $\log_{10}$ CFU/ml for isoniazid, whereas that for rifampin was 5.30 to 5.68 $\log_{10}$ CFU/ml, after 7 days of coincubation (Fig. 2, A to C). Neither ceftazidime nor avibactam alone killed *Mtb*, even a little (Fig. 2, D and E). However, the combined CAV killed *Mtb* with an E_{max} of 4.19 to 7.05 $\log_{10}$ CFU/ml, exceeding isoniazid and pyrazinamide and equaling rifampin, at concentrations that are clinically achievable (Fig. 2, F and G). A repeat study of ceftazidime concentration combined with avibactam at a concentration of either 0, 1, 5, or 15 mg/liter revealed that a minimum avibactam concentration of 1 mg/liter was needed to confer the ceftazidime microbial kill. Because neither ceftazidime alone nor avibactam alone killed *Mtb*, but CAV did (Fig. 2, F and G), the reason for the poor activity of ceftazidime against *Mtb* is not the lack of a penicillin-binding protein target but β-lactamase activity.

Drug-resistant *Mtb* clinical isolates are susceptible to CAV

Next, we determined how widespread the CAV susceptibility is among *Mtb* isolates, using two MIC assays. Five laboratory isolates had identical MICs in microbroth dilution and Mycobacteria Growth Indicator Tube BACTEC (MGIT) assays, at MICs shown in Fig. 2H. Next, we used the MGIT assay to identify MICs for 25 clinical strains from South Africa, which included 80% X/MDR-TB strains representing all known *Mtb* phylogenetic lineages. We identified the MIC distribution shown in Fig. 2H. This shows that the MICs of 24 of the 25 (96%) clinical strains were below the CAV peak concentrations of 90 to 100 mg/liter, achieved with therapeutically achievable concentrations at standard doses. Thus, most clinical strains from X/MDR-TB patients were susceptible to CAV.

## CAV human-like intrapulmonary pharmacokinetics have high bactericidal effects

The HFS-TB allows us to perform dose-response studies using concentration-time profiles of antibiotics at the site of infection. We used the HFS-TB of log-phase *Mtb* H37Ra to recapitulate the intrapulmonary concentration-time profiles of seven CAV doses using the same commercially available CAV formulation (ceftazidime/avibactam ratio of 4:1) administered every 8 hours for 27 days; each infusion was administered over 2 hours, on the basis of pharmacokinetics reported to the FDA and EMA for licensing purposes, and had a half-life of 3.3 hours (13, 14, 21). We measured the CAV concentrations in each HFS-TB, and pharmacokinetic modeling confirmed the half-life of 3.3 hours. Figure 3A shows that CAV achieved marked microbial kill of the log-phase growth *Mtb* at bactericidal effect kill rates higher than standard dose isoniazid, pyrazinamide, and rifampin monotherapy with drug-susceptible *Mtb* in the HFS-TB in the past (18, 22, 23). Figure 3A shows an unprecedented effect in the HFS-TB, which is 6.0 $\log_{10}$ CFU/ml kill in just 7 days; the most effective first-line drugs of isoniazid and rifampin have a kill of <2.0 $\log_{10}$ CFU/ml over the same time period in the same HFS-TB model and in sputum of patients (15, 22, 23). Thus, at a minimum, CAV administered with human-like pharmacokinetics demonstrated a bactericidal effect exceeding that of first-line drugs as monotherapy and in combination.

## CAV therapeutic exposure targets are time-dependent

Next, we wanted to identify the dosing schedule and optimal concentrations or exposures (defined as concentration/MIC) that are associated with maximal microbial kill and resistance suppression. We used a dose-fractionation design and a slightly faster half-life, which allowed us to examine the effects of different dosing schedules and exposure patterns by breaking colinearity that would accompany dose changes, as shown in the drug concentration–time profiles we measured in each HFS-TB in Fig. 3 (B to D). We achieved a half-life of 2.6 ± 0.3 hours (r^2 = 0.99). Figure 3 (B to D) shows that the percentage of time (24 hours) that CAV concentration persisted above MIC (%T_{MIC}) was lowest with the once-a-day dosing schedule, followed by twice a day, although the peak concentrations were the same despite dosing schedule. Thus, we achieved the experimental design objective. The effect on *Mtb* burden was assessed using two methods: determining CFU per milliliter (CFU/ml), which is commonly used in the research laboratory, and determining time to positivity (TTP) in the MGIT, which is more commonly used by clinicians and correlates with long-term treatment outcomes (24, 25). On the basis of the Akaike information criteria scores for exposure versus bacterial burden model fits, the %T_{MIC} was the best driver of microbial kill by both CFU/ml and TTP, better than peak-to-MIC and area under the concentration-time curve to MIC (AUC/MIC). This means that the CAV effect against *Mtb* will be optimized by the three-times-a-day dosing schedule, and the once-a-day dosing schedule would kill less. Figure 3E and fig. S1 show these exposure-effect relationships between %T_{MIC} and *Mtb* burden for each sampling day. We used these exposure-effect relationships to calculate the CAV exposure that would achieve the same kill rates in the HFS-TB and in the sputum of patients as those of the first-line drugs, which are 1.95 $\log_{10}$ CFU/ml (or 0.28 $\log_{10}$ CFU/ml per day) for rifampin, 1.8 $\log_{10}$ CFU/ml (or 0.6 $\log_{10}$ CFU/ml per day) for isoniazid during the first 7 days, and 0.10 $\log_{10}$ CFU/ml per day after the first 4 days for pyrazinamide (15, 18, 22, 23, 26, 27). The CAV exposure that achieved the same kill rates as those of the most active of the first-line drugs was a %T_{MIC} of ≥47%. We also calculated the CAV exposure associated with maximal kill, which was a %T_{MIC} of ≥63%. Therefore, CAV has to be dosed at exposures exceeding a %T_{MIC} of 63% (that is, 63 to 100%) for optimal efficacy. Exposure target values are known to be the same between the HFS-TB and TB patients (8, 27, 28). Thus, the %T_{MIC} values of 47 and 63% are the exposure targets that must be achieved or exceeded by CAV doses in patients to achieve the same amounts of microbial kill in patients, as was observed in the HFS-TB (8, 27, 28).

We also modeled the size of the drug-resistant subpopulation (CFU/ml), captured using CAV concentration of six times MIC on agar (18, 28). The size of the drug-resistant subpopulation was driven by the AUC/MIC ratio achieved, as shown in Fig. 3F, with suppression of acquired drug resistance at an AUC/MIC ratio of 250. We collected 12 of the CAV-resistant isolates, confirmed that they grew at a CAV concentration of 96 mg/liter in broth, and then extracted DNA for WGS. We identified 149 single-nucleotide variants (SNVs) common to the 12 CAV-resistant isolates not present in the wild type, shown in table S1. The nonsynonymous SNVs are shown in Fig. 4. Excluding the mutations in the highly polymorphic genes encoding proteins carrying proline–glutamic acid (PE) or proline–proline–glutamic acid (PPE) motif, there were a total of 53 genes with at least one SNV, mostly in genes encoding cell wall and membrane components and processes. The most notable SNVs included genes encoding the bifunctional penicillin-binding protein *ponA1* (average coverage of 192 times) transpeptidase domain, *rpfE* (average coverage of 200 times) encoding *Mtb*'s lytic transglycosylase, and secretion system genes. In several resistant isolates (but not all), there was also a mutation in *rpfA*, which encodes the lytic transglycosylase. Notably, there were no mutations in *blaC*, Ldt_{Mt1}, and Ldt_{Mt2} (average coverage of 125 times). We confirmed the lack of mutations in *blaC*, Ldt_{Mt1}, and Ldt_{Mt2} in a second DNA extraction of the strains using Sanger sequencing.
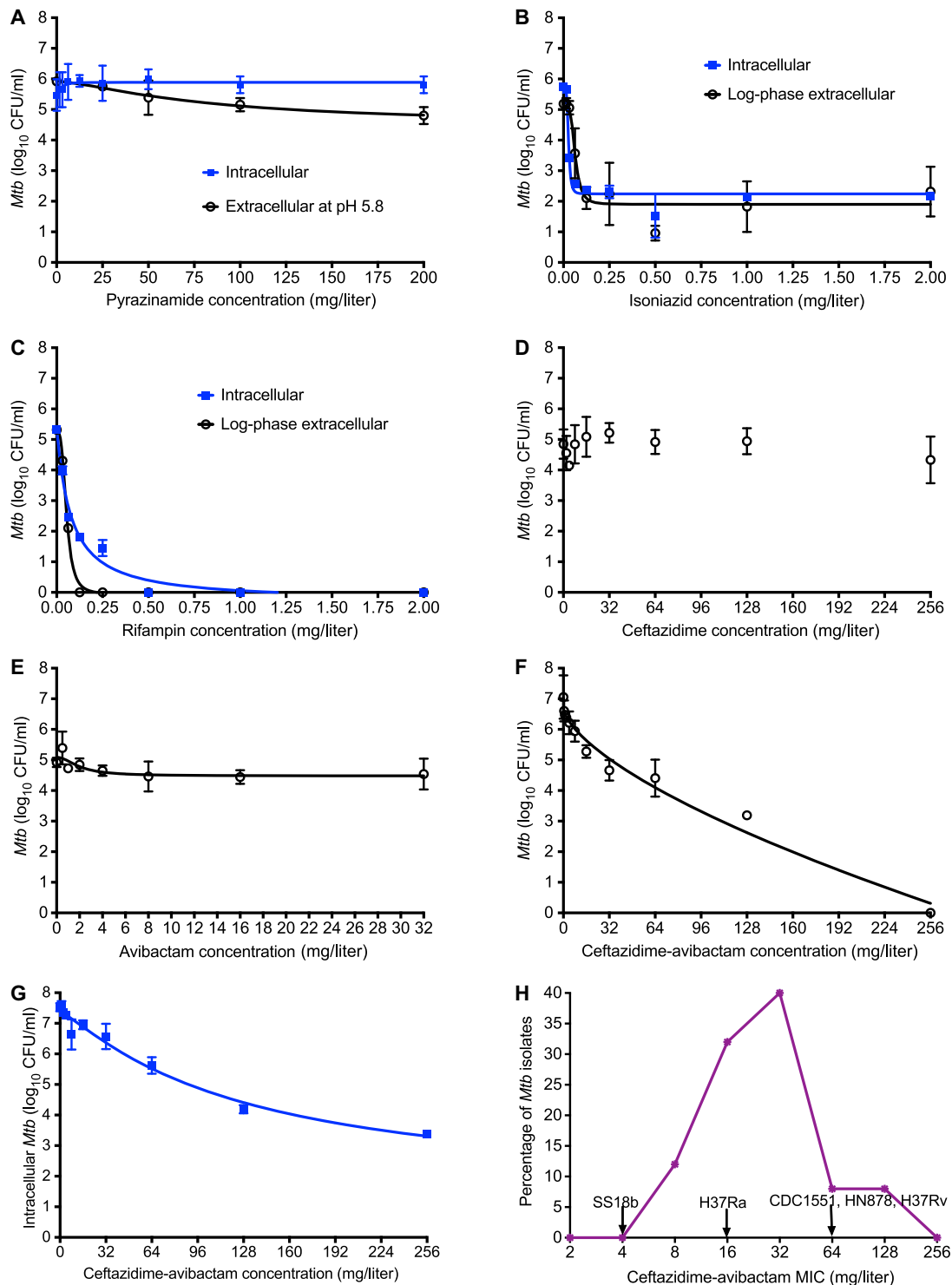
Fig. 2. Exposure effect screening study of CAV against *Mtb*. Each concentration was examined in triplicate, and results shown are for mean and SD (error bar). For each study, concentration versus $\log_{10}$ CFU/ml was examined using the inhibitory sigmoid E_{max} model. (**A**) Pyrazinamide failed to kill intracellular *Mtb* in 7 days. We acidified broth, which enabled pyrazinamide to kill *Mtb* but had poor fit of the model to the data ($r^2 = 0.718$), associated with maximal kill (E_{max}) of 1.43 ± 1.07 $\log_{10}$ CFU/ml. (**B**) Isoniazid E_{max} was 3.56 ± 0.10 $\log_{10}$ CFU/ml against intracellular *Mtb* ($r^2 = 0.988$), similar to the E_{max} of 3.32 ± 0.33 $\log_{10}$ CFU/ml ($r^2 = 0.845$) for extracellular *Mtb*. (**C**) Rifampin E_{max} for intracellular *Mtb* was 5.68 ± 0.30 $\log_{10}$ CFU/ml ($r^2 = 0.976$), and that for extracellular bacteria was 5.30 ± 0.09 $\log_{10}$ CFU/ml ($r^2 = 0.996$). (**D**) Ceftazidime alone did not kill *Mtb*. (**E**) There was also poor fit of the model to the data for avibactam because of minimal to no microbial kill by the avibactam ($r^2 = 0.357$). (**F**) CAV achieved an E_{max} of 7.05 ± 0.00 $\log_{10}$ CFU/ml and an EC_{50} (median effective concentration) of 104.50 ± 13.44 mg/liter ($r^2 = 0.910$) against extracellular *Mtb*. This EC_{50} is easily achieved with standard doses. (**G**) CAV achieved an E_{max} of 4.19 ± 0.29 $\log_{10}$ CFU/ml and an EC_{50} of 74.92 ± 9.03 mg/liter ($r^2 = 0.960$) against intracellular *Mtb*. (**H**) CAV MICs for five laboratory isolates are shown by arrows. The modal MIC in clinical isolates was 32 mg/liter.
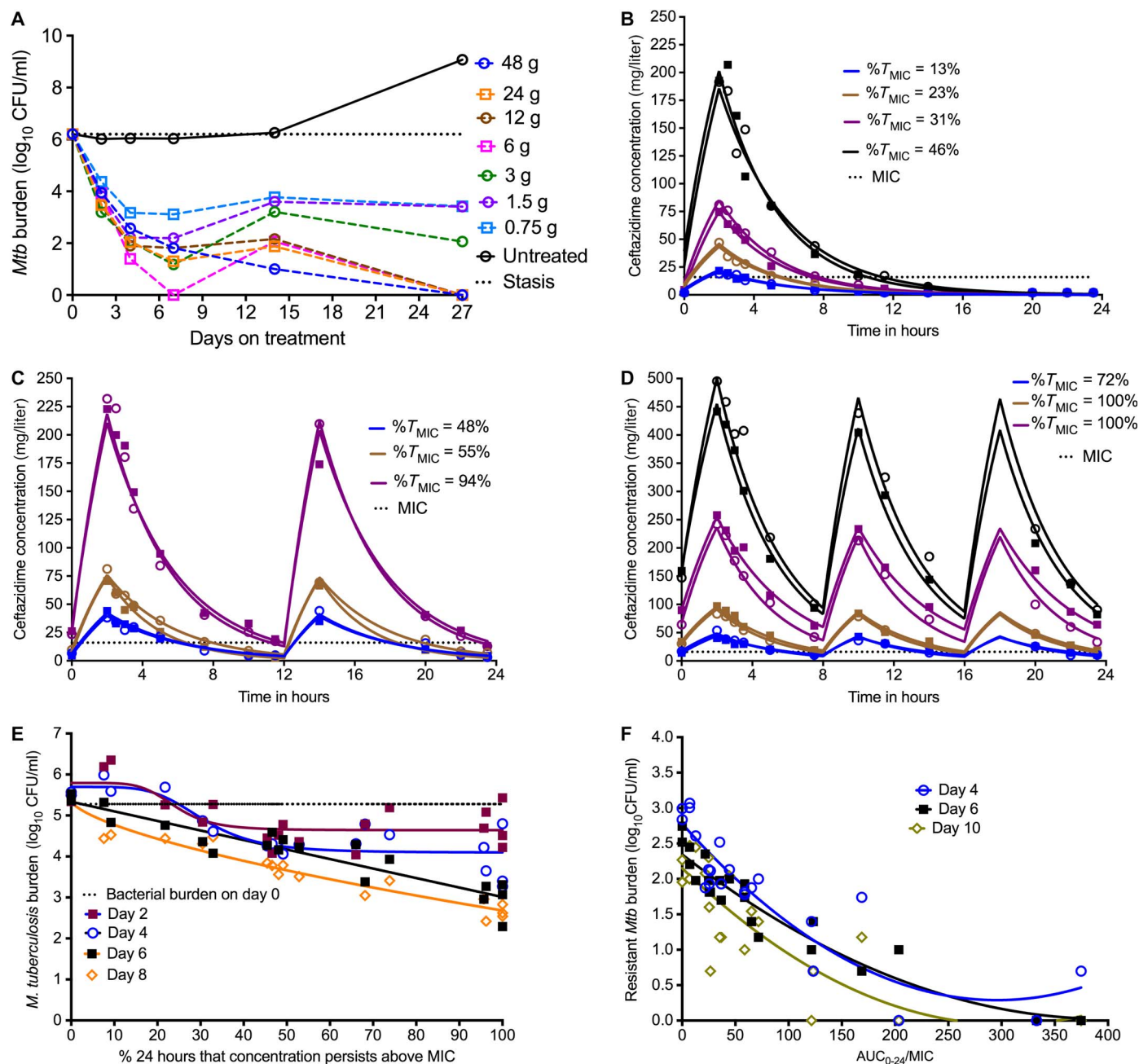
Fig. 3. Bactericidal effect of CAV in the HFS-TB. Data for each unit in replicate HFS-TB are shown separately. (**A**) In the first HFS-TB study, CAV was administered three times per day to each HFS-TB system, to produce concentration-time profiles similar to the stated human doses. The lowest human equivalent dose of 0.75 g demonstrated significant kill below the day 0 bacterial burden (stasis) of 2.78 $\log_{10}$ CFU/ml. At a dose of 6 g, the day 0 burden of 6.2 $\log_{10}$ CFU/ml was reduced to 0, indicating marked speed of bactericidal effect that is greater than isoniazid's 1.8 $\log_{10}$ CFU/ml in the HFS-TB and in patients, which is the most effective first-line drug against log-phase growth *Mtb*. (**B** to **D**) In the second HFS-TB study, triplicate HFS-TBs were treated with CAV in a dose-fractionation design. Concentration-time profiles achieved with once-a-day dosing schedule (B) had the lowest proportion of time above MIC (%T_{MIC}), compared to the twice-a-day dosing schedule (C) that had matching peak concentrations; %T_{MIC} was highest with the dosing schedule of every 8 hours (D). (**E**) The inhibitory sigmoid E_{max} model for CFU/ml versus %T_{MIC} had an r^2 of 0.94 on day 8. (**F**) The relationship between AUC/MIC and CAV-resistant CFU/ml had an r^2 of 0.90; the ratio associated with resistance suppression can be read off the graph as a ratio of 250.

Both ceftazidime and avibactam are highly concentrated inside *Mtb*-infected cells

To determine whether CAV would be effective against intracellular *Mtb*, we infected THP-1 monocytes with *Mtb*, as described above, and then inoculated them into HFS-TB conditioned with RPMI and 2% fetal bovine serum (FBS) (*19, 20*). HFS-TB replicates were then treated with CAV

daily for 26 days, which we confirmed by repetitive sampling of both the central compartment (systemic concentrations) and *Mtb*-infected monocytes. Figure 5A shows the concentrations of ceftazidime and avibactam achieved inside the *Mtb*-infected monocytes: The concentrations achieved by both drugs at all time points were much higher inside the monocytes than extracellularly. Thus, all CAV-treated systems achieved
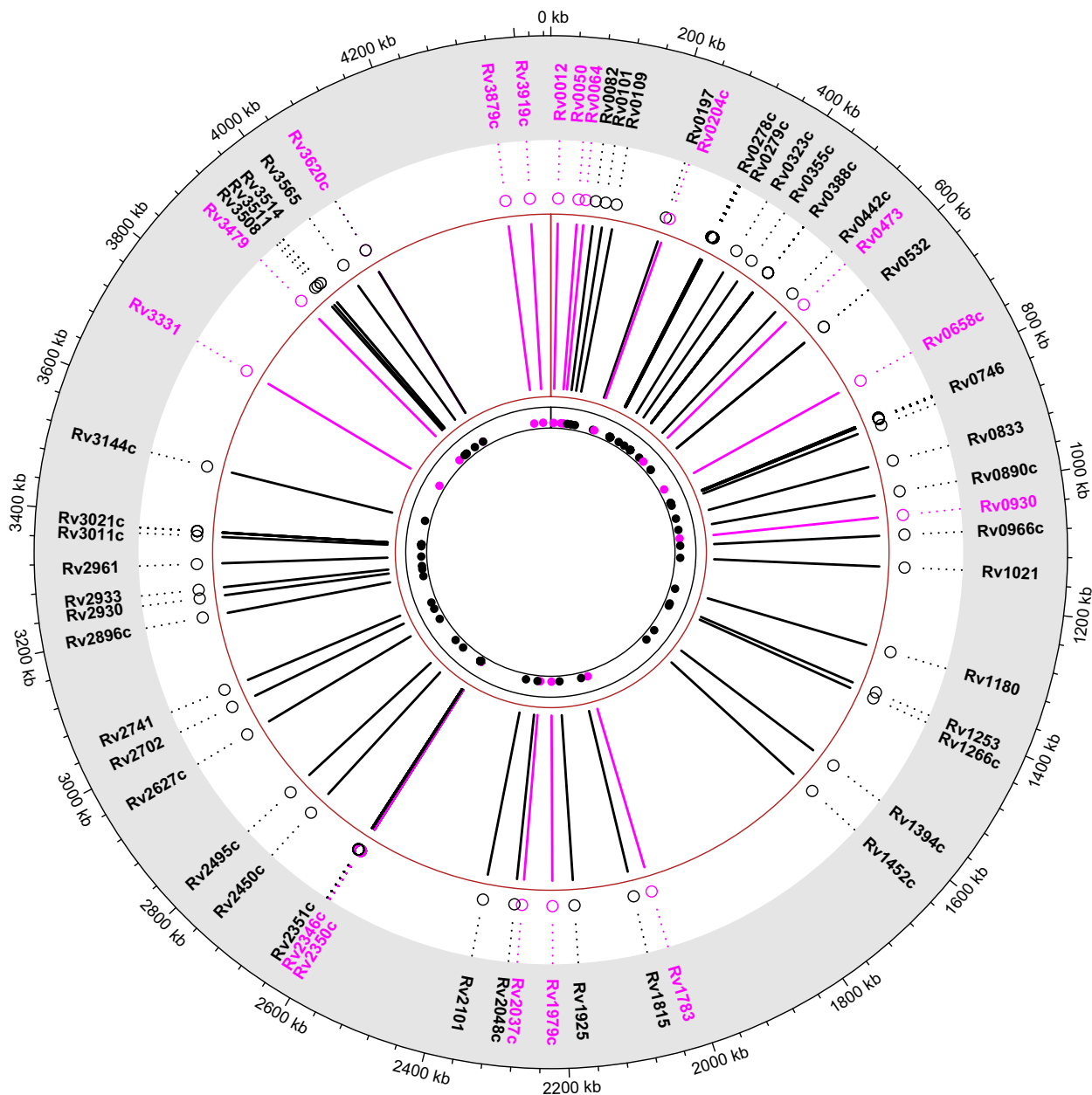
Fig. 4. Mutations in the *Mtb* genome of resistant mutants. Shown are the mutations that were common to all 12 drug-resistant isolates. Cell wall and cell membrane component genes are in magenta, including those for *Rv0012* (PonA1).

a %T_{MIC} of 100% both extracellularly and intracellularly. Microbial kill results based on TTP are shown in Fig. 5B, showing that the CAV mono-therapy increased TTP >2-fold from day 0. Figure 5C shows that *Mtb* in untreated control HFS-TB replicates grew at an average rate of 0.119 log$_{10}$ CFU/ml [95% confidence interval (CI), 0.051 to 0.186], with maximal growth rate of 0.293 log$_{10}$ CFU/ml (95% CI, 0.156 to 0.429) in the first 10 days. Figure 5C further demonstrates that in the CAV-treated HFS-TB replicates, microbial kill was 3.0 log$_{10}$ CFU/ml below that of day 0, and with a difference of >5 log$_{10}$ CFU/ml with untreated controls. This kill rate magnitude is in the same range as that of the three first-line drugs combined in the same HFS-TB model in the past (*29*). These results mean that CAV kills the intracellular *Mtb* subpopulation and has the advantage of high intracellular penetration.
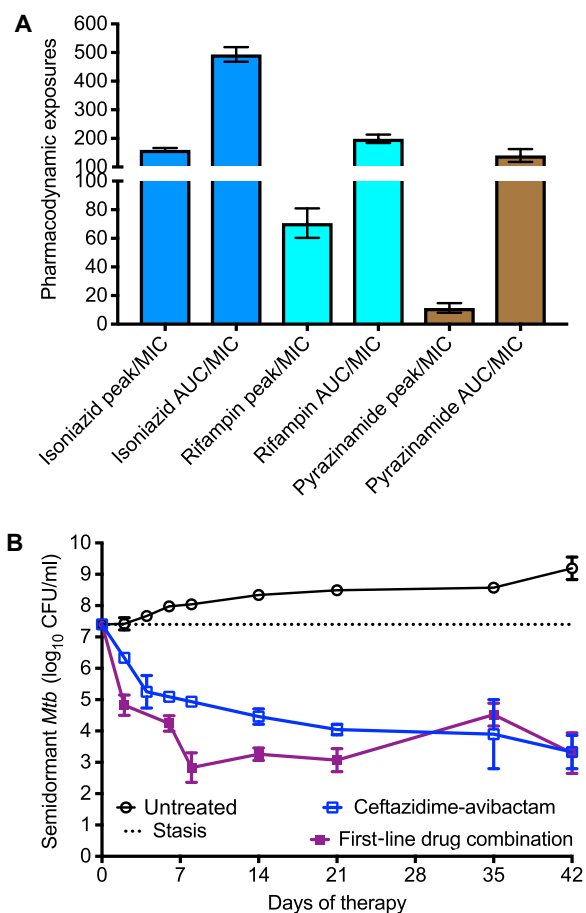
CAV sterilizing effect is similar to that of the three first-line drugs in combination

Next, we wanted to compare the sterilizing effect of CAV monotherapy to the first-line drug combination (isoniazid, rifampin, and pyrazin-amide). We used the HFS-TB model of extracellular semidormant *Mtb* H37Rv, in broth acidified to pH 5.8 (*18*), treated three times daily for 6 weeks. The drug concentrations we measured and the exposures achieved in each replicate HFS-TB are shown in Fig. 6A. Because a %T_{MIC} of 100% and the exposures of first-line drugs achieved are those associated with optimal microbial kill for each, we compared the best possible sterilizing effect of CAV to the best of the first-line drug combina-tion. Figure 6B shows that untreated controls grew very slowly in this HFS-TB model, at a rate of 0.026 log$_{10}$ CFU/ml (95% CI, 0.009 to 0.04), which
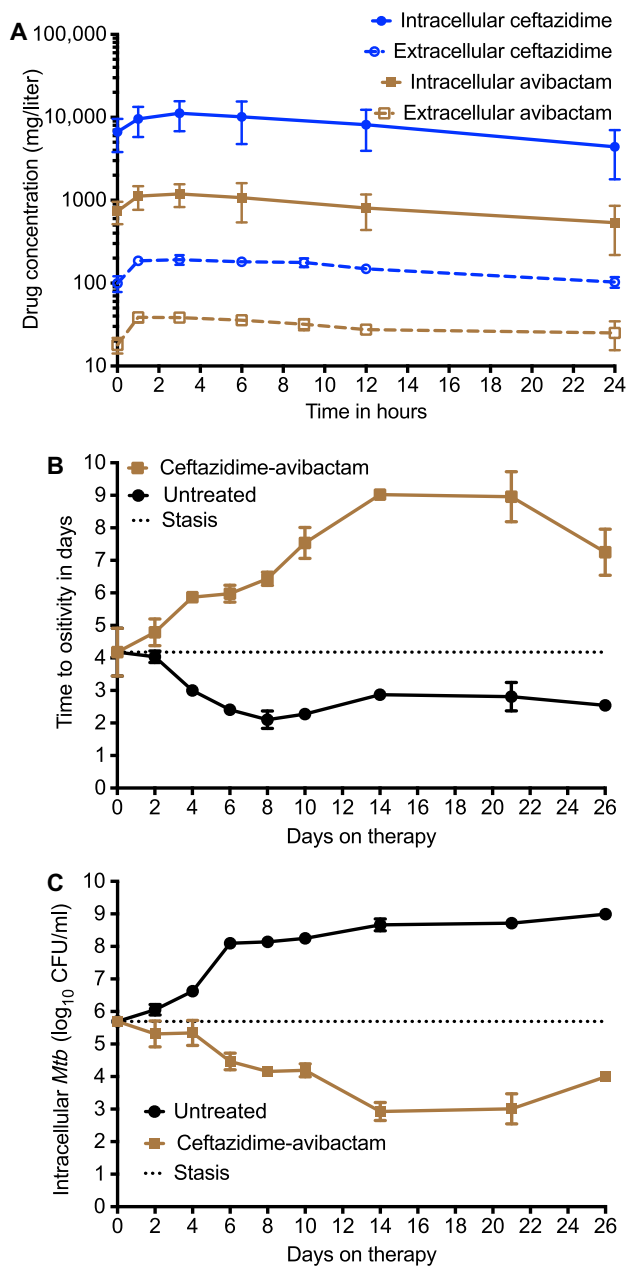
Fig. 5. Pharmacokinetics and efficacy of CAV in intracellular *Mtb*. Mean values and SDs (error bars) are shown in three replicates each. Given the range of concentrations, we used a $\log_{10}$ scale for drug concentrations and intracellular to extracellular ratios for pharmacokinetic parameters and concentrations. (**A**) There were much higher concentrations achieved for both avibactam and ceftazidime inside the infected monocytes compared to those outside. (**B**) TTP increased 2.2-fold (maximal) on CAV alone, consistent with decreased bacterial burden. (**C**) *Mtb* CFU/ml reveals ~3.0 $\log_{10}$ CFU/ml decline below day 0 burden with CAV treatment.

Fig. 6. Sterilizing effect of CAV versus standard combination therapy. We compared the sterilizing effect of CAV to standard first-line drug combination in three replicates of hollow fiber systems for each treatment condition. Standard therapy consists of rifampin, isoniazid, and pyrazinamide, with ethambutol added in the beginning in case there is isoniazid resistance, and is dropped when susceptibility results become available; with some new point of care diagnostics, isoniazid susceptibility is actually known quickly, and ethambutol was excluded. In the figures, the mean value is shown with SD error bars. On many sampling days, the error bars were too small (SD was very low) and are obscured by the symbol. (**A**) First-line drug exposures achieved in the replicate HFS-TB. The MICs were 0.125 mg/liter for rifampin, 0.06 mg/liter for isoniazid, and 12.5 mg/liter for pyrazinamide, in *Mtb* H7Rv. (**B**) The mean *Mtb* burden progressively declined throughout the course of treatment with CAV to a kill of 4.72 $\log_{10}$ CFU/ml below stasis (day 0 bacterial burden) at the end of the study on day 42. It can also be seen that starting on day 35, the CAV effect was similar to the standard three-drug regimen.

ment on day 42, the CAV monotherapy had killed exactly the same as the first-line drug combination. Thus, CAV monotherapy may have a sterilizing effect that is only slightly less than that of the three-drug first-line drug combination.

Treatment of X/MDR-TB and incurable TB would be achieved with doses tolerated by patients

The main drivers of therapeutic outcomes in TB patients are pharmacokinetic variability and *Mtb* isolate MICs (*31–37*). The translational pathway that starts with HFS-TB findings, followed by Monte Carlo simulations that take into account the pharmacokinetic and MIC variability, has a quantitative forecasting accuracy of 94% for identified optimal doses and susceptibility breakpoints (*8, 28*). Exposure target

is 11.27 times slower than the intracellular population and is in the expected range for semidormant bacilli (*30*). There was a biphasic decline in CFU/ml with CAV monotherapy treatment, a 2.3 $\log_{10}$ CFU/ml decline during the first week, followed by a slower decline, which was nevertheless sustained for up to 6 weeks. The microbial kill by the standard three-drug combination therapy, although better than that of the CAV monotherapy, was only marginally so. By the end of the experi-

values are known to be the same between the HFS-TB and TB patients; thus, the same exposure targets of a %T_{MIC} of either 47 or 63% were used to translate CAV efficacy from the laboratory to the clinic (8, 27, 28). To identify the CAV clinical dose that would achieve or exceed the exposure target in >90% of 10,000 TB patients, we entered the population pharmacokinetic parameter estimates of CAV and their interindividual variability in children and in adult TB patients, as well as the lung penetration ratios (13, 38–40), in subroutine PRIOR of ADAPT software (table S2). Each of the computational steps for the simulations was outlined in detail in Materials and Methods. We validated the clinical trial simulations using steps we previously described in detail (28).

Our simulations identified the ceftazidime and avibactam concentrations for the standard CAV dose of 50 mg/kg in 10,000 young children (Fig. 7A), which was similar to those identified in the clinic with that dose (38). This means that the simulation accurately achieved drug concentrations achieved by specific doses in the children. For the exposure target %T_{MIC} of 47%, which gives similar microbial kill as the most active standard first-line drugs, CAV doses of 50, 100, 150, and 200 mg/kg infused over 2 hours every 8 hours achieved or exceeded the target at each

MIC in proportions of children shown in Fig. 7B. More than 90% of the children treated with a CAV dose of 50 mg/kg achieved this exposure target in *Mtb* isolates with an MIC of up to 32 mg/liter, 90% of those treated with a CAV dose of 100 mg/kg achieved the target with an MIC of up to 64 mg/liter, whereas 90% of the children treated with CAV doses of 150 to 200 mg/kg achieved or exceeded the target with an MIC of up to 128 mg/liter. In the HFS-TB, a CAV %T_{MIC} of 63% actually kills 11 times more than isoniazid monotherapy, which could shorten therapy duration. Figure 7C shows the target attainment for the %T_{MIC} of 63% in children treated with the same four doses: The MICs, above which target attainment falls to less than 90%, were one tube dilution lower than the %T_{MIC} of 47% target. Figure 7D is a summation over the entire MIC range for the clinical isolates from South Africa and is the proportion of 10,000 children who achieved each of the two exposure targets. Figure 7D shows that the dose of 100 mg/kg, which has been shown to be tolerated by children (40), would achieve exposures that kill as well as the first-line anti-TB drugs in 90% of the children and would also achieve kill rates faster than those for the first-line drugs in 60% of the children. Simulations of 10,000 children patients for the avibactam component revealed
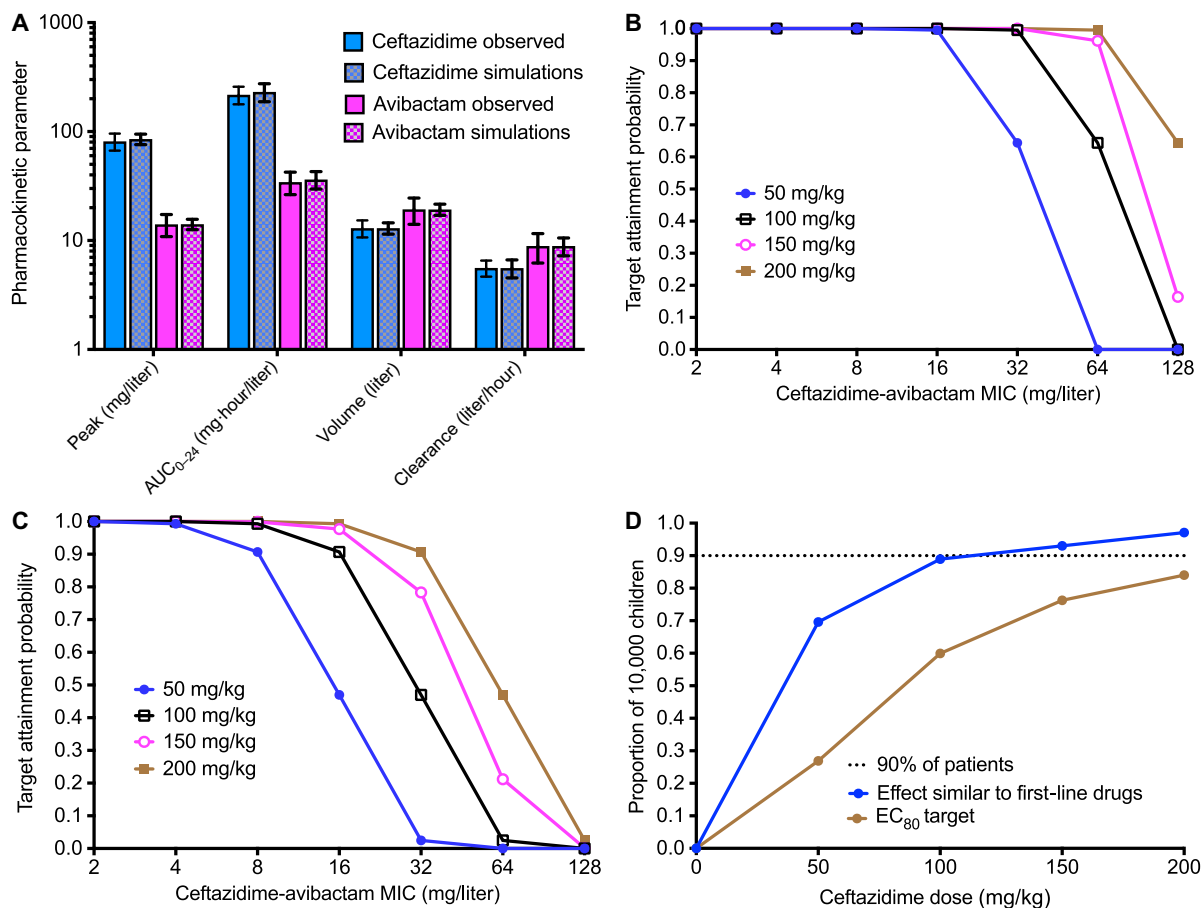
Fig. 7. CAV dose target attainment in childhood TB. Each data point is shown as the proportion of 10,000 children. (**A**) Pharmacokinetic parameters and concentrations of ceftazidime and avibactam in 10,000 simulated children treated with a CAV dose of 50/12.5 mg/kg are compared to those observed in the clinic in children treated with this same dose for other indications. Our simulated children achieved concentrations that are the same as those that were observed in the clinic by others (used here to benchmark), meaning that the simulations faithfully recapitulated concentrations that are achieved in children by the different doses. (**B**) The dose of 100 mg/kg achieved good target attainment for %T_{MIC} of 47% up to an MIC of 64 mg/liter. (**C**) For the %T_{MIC} 63% target, only the dose of 200 mg/kg achieved good target attainment up to an MIC of 64 mg/liter. (**D**) A summary of the proportion of 10,000 children with TB who achieved each of the two target %T_{MIC} values of 47 and 63% over the entire MIC range for each dose. The dose of 100 mg/kg achieves the target that gives the same kill rates as standard first-line drugs in 90% of the children and even higher kill rates in at least 60% of the children. This means that the dose of 100 mg/kg is recommended for clinical testing in children with TB.

that all tested doses achieved the target of 1 mg/liter of avibactam over both 47 and 63% of dosing interval, when administered as the commercially available CAV combination that has a ceftazidime/avibactam ratio of 4:1.

We performed similar Monte Carlo experiments for adult cavitary TB, in which 80% of *Mtb* is extracellular (*16*); patients have tolerated seven to eight times the standard 2-g dose even as a continuous infusion in the past (*39*, *40*). Figure 8A shows that concentrations achieved in our 10,000 simulated adult patients were similar to those reported in the FDA docket in patients treated with a 2-g dose three times a day. Therefore, our simulations accurately recapitulated concentrations achieved by the specific doses in the clinic. Figure 8B shows that for exposure target of %T_{MIC} of 47%, the target attainment was achieved in >90% of the patients with *Mtb* isolates that had CAV MICs of ≤16 mg/liter for standard 2-g dose and MICs of up to 64 mg/liter for 12-g dose a day. Figure 8C shows that the more stringent exposure target of %T_{MIC} of 63% was more difficult to achieve, at each MIC, in adults than in chil-

dren. Figure 8D shows the proportion of 10,000 adult TB patients who would achieve each of the two exposure targets over the entire MIC range; the graph flattens out after 12 g for the %T_{MIC} of 47% target. Therefore, 12 g is the dose to be used as salvage therapy in adult TB. With regard to avibactam, all doses tested achieved the target of 1 mg/liter of avibactam over 47% of dosing interval. In summary, we identified a CAV dose of 100 mg/kg in children, and 12-g dose a day in adults would achieve kill rates similar to rifampin; 60% of children actually exceed that kill rate.

DISCUSSION

We found that CAV has remarkable sterilizing effect at clinically achievable concentrations. Neither ceftazidime nor avibactam on its own killed *Mtb*, but the combined formulation did. This suggests that the natural resistance of *Mtb* to ceftazidime is via degradation of the drug and not because *Mtb* does not have the cephalosporin's target. *blaC* is
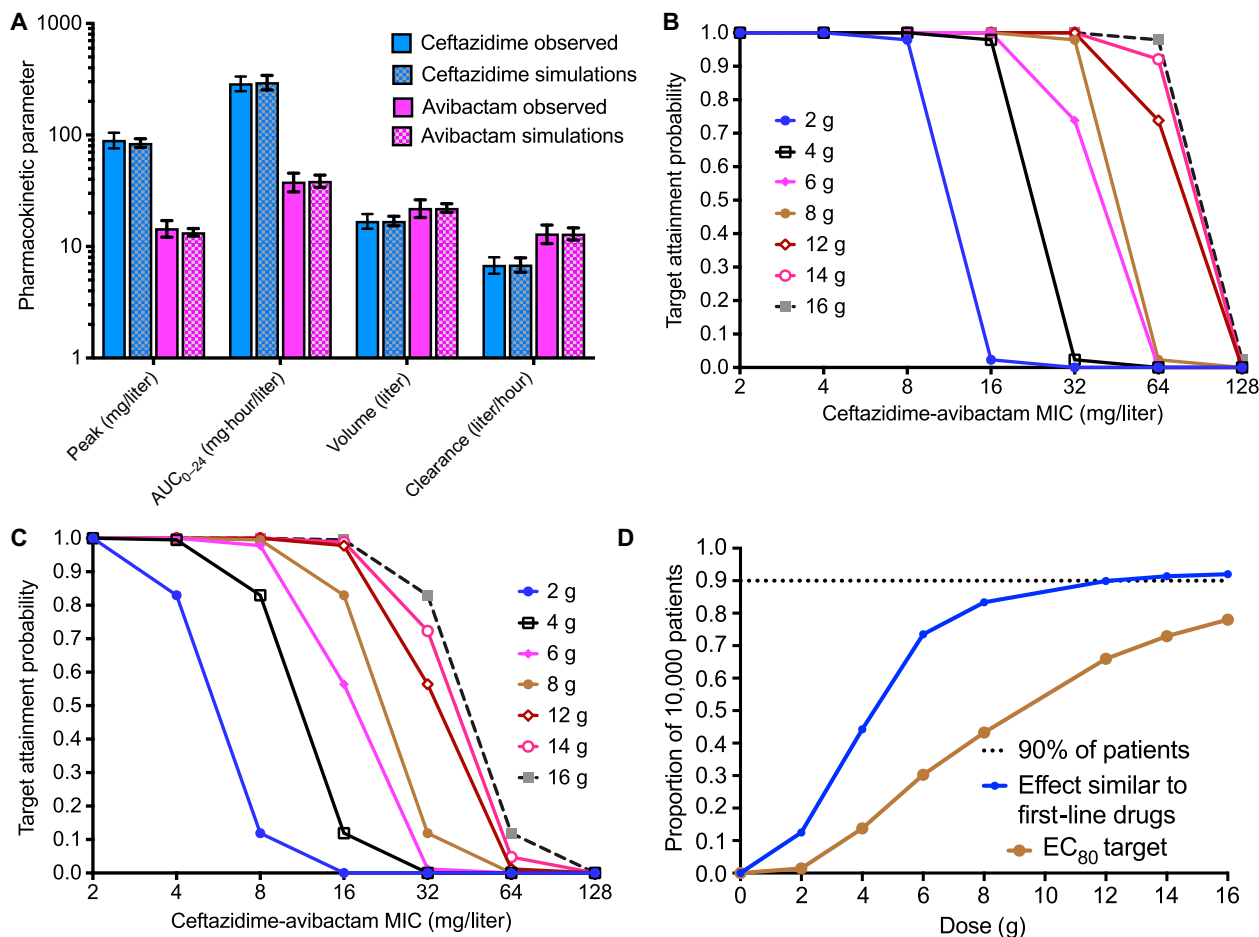
Fig. 8. CAV dose target attainment in adult-type TB. Each data point is shown as the proportion of 10,000 adult patients. (**A**) To validate that the simulations reflected clinical reality, we compared the pharmacokinetic parameters of clearance and volume, as well as drug concentrations such as peak and AUC concentrations achieved in the 10,000 simulated patients treated with the CAV dose of 2000/500 mg, to those observed in clinical pharmacokinetic studies published by others. It can be seen that the values in the simulated subjects are almost exactly the same as those observed in actual patients by others, meaning that the simulations worked. (**B**) The proportion of patients at each MIC who achieved a %T_{MIC} of 47%, termed target attainment probability, in simulated subjects treated with doses between 2 and 16 g. As MIC increases, the target attainment probability falls, but higher doses perform better until a dose of 12 g, above which there is no further improvement. (**C**) Target attainment probability for the %T_{MIC} target of 63% was poor for all doses examined in adults. (**D**) Proportion of 10,000 adult TB patients treated with different doses who achieved %T_{MIC} of 47 or 63% over the entire MIC range for each dose. The dose of 12 g achieves the target that gives the same kill rates as standard first-line drugs in 90% of the patients. This means that the dose of 12 g is recommended for clinical testing in adults with TB.

the lone gene that encodes a β-lactamase in *Mtb* (*41*). *Mtb* BlaC shows broad activity against cephalosporins such as ceftazidime; however, clavulanate is a relatively poor inhibitor of this enzyme (*42*). In contrast, avibactam is an effective BlaC inhibitor. However, none of our 12 resistant isolates harbored a *BlaC* mutation. Instead, all 12 CAV-resistant isolates harbored both a PonA1 Prol631Ser and an RpfE Arg126Gln nonconservative mutation. *ponA1* encodes penicillin-binding protein 1 (PBP1), a bifunctional enzyme with a C-terminal transpeptidase in residues 561 to 820, catalyzing (D,D) 4→3 linkages in peptidoglycan synthesis and with a hydrolytic N-terminal domain transglycosylase (*43*). The mutations in these genes in CAV-resistant isolates suggest that PBP1 could be a putative site for CAV binding. CAV-resistant isolates also had *rpfA* and *rpfE* mutations, encoding resuscitation protein factors. *Mtb*'s five resuscitation protein factors share a lytic transglycosylase domain and hydrolyze glycan chains in peptidoglycan. One of these, rpfB, forms a complex with the endopeptidase RipA, which synergistically hydrolyses peptidoglycan; this hydrolysis action by the complex is inhibited by PBP1 (*43*, *44*). RipA also interacts with rpfE, which shares 66% identity with rpfB (*44*). The *rpf* mutations further suggest CAV interference with peptidoglycan synthesis. However, our findings are not definitive and only give a plausible hypothesis of the ceftazidime *Mtb* target; thus, more detailed biochemical work will be needed to confirm our hypothesis.

In the global fight against TB, we have run out of options for the treatment of many patients. Despite the recent introduction of bedaquiline and delamanid in high–TB burden countries, there continues to be a large number of patients with incurable TB. We found that CAV, which is already commercially available as a combined formulation, is likely to be useful as salvage therapy for patients with difficult-to-treat TB: It can also be added to bedaquiline and delamanid. Use of CAV circumvents the need to use amoxicillin-clavulanate in conjunction with injectable β-lactams and the attendant common side effects. In addition, the 9-month MDR-TB treatment regimen recently announced by the World Health Organization includes aminoglycosides as an important part of the regimen. These injectables are associated with hearing loss of up to 70% in some of adult patients and in up to 25% of children (*45*, *46*). CAV could be a less toxic alternative and arguably more effective. In addition, CAV could be safer for use in neglected TB populations, such as pregnant women, for which anti-TB drugs with minimal teratogenicity are needed. Finally, CAV has no known interactions with antiretroviral agents and can thus be used in HIV/TB co-infection.

We identified a CAV dose of 100 mg/kg three times a day for use in the treatment of TB of children, and up to 12 g in adults, as optimal. Patients have tolerated avibactam doses of up to 2000 mg and ceftazidime doses of up to 200 mg/kg as a continuous infusion in the past (*38–40*). However, given that long-term administration would be required to treat TB, the full side effect profile over longer treatment durations is unknown and will require careful documentation. Nevertheless, given the urgent need, the dose and dosing schedule should be tried as salvage therapy in patients who have no other treatment options. We also identified a CAV susceptibility breakpoint of 128 mg/liter for *Mtb*. This remains to be validated in the future; however, the approach we used on HFS-TB findings followed by Monte Carlo simulations has identified susceptibility breakpoints for rifampin, isoniazid, and pyrazinamide, which were later confirmed in clinical studies (*34–37*). This is also likely in the case of CAV.

Finally, we introduce a paradigm for rapid screening of different antibiotics for effect against *Mtb*, examining susceptibility in X/MDR-TB strains and then quickly taking promising candidates through steps to identify optimal doses. This approach takes months rather than years and could

alleviate the current crises while new anti-TB molecules are being developed. These medications, such as CAV, could be rapidly advanced to clinical testing and to use as salvage therapy.

MATERIALS AND METHODS
Bacterial strains and cell lines
The following laboratory *Mtb* strains were used in the experiments: H37Ra [American Type Culture Collection (ATCC) #25177], H37Rv (ATCC #27294), CDC 1551, HN878, and *Mtb* 18b (donated by S. Cole). The 25 clinical strains from TB patients were collected by the Medical Research Council of South Africa. Human-derived THP-1 cells (ATCC TIB-202), grown in RPMI 1640/10% FBS, were infected with H37Ra, as described previously (*19*, *23*, *29*). All studies with virulent Mtb strains were performed in a BSL3 laboratory.

Materials and drugs
Ceftazidime and CAV were purchased from the Baylor University Medical Center pharmacy. Avibactam was purchased from BOC Sciences. Hollow fiber cartridges were purchased from FiberCell.

Human and animal subjects
No human or animal studies or experiments were performed.

Determination of MICs
CAV (4:1 ratio) MICs were examined using the final ceftazidime concentrations of 0, 1, 2, 4, 8, 16, 32, 64, 128, and 256 mg/liter, in triplicate. In the MGIT, the lowest concentration of CAV that prevented the drug-containing tube from fluorescing within 2 days of the drug-free tube or control was defined as the MIC.

Hollow fiber system model of TB
In the HFS-TB experiments, 20 ml of *Mtb* cultures, preconditioned either at pH 6.8 or 5.8 or in infected THP-1 cells, is inoculated into peripheral compartments of HFS-TB preconditioned for 72 hours (*18*, *19*, *22*). In the dose-effect study, CAV was administered at ceftazidime-to-avibactam human equivalent doses of 0, 0.75 to 0.1875, 1.5 to 0.375, 3.0 to 0.75, 6.0 to 1.5, 12.0 to 3, 24.0 to 6, and 48.0 to 12 g for 27 days. Each drug infusion was over 2 hours. CAV concentration-time profiles achieved in each HFS-TB were validated by sampling the central compartment of each system at 0-, 1-, 4-, 7-, 9-, 12-, and 23-hour time points. CAV drug concentration assays were described in "CAV drug assay." The peripheral compartments were sampled on days 0, 1, 2, 4, 7, 10, 14, 21, and 27 for quantification of *Mtb*. In the dose-fractionation experiments, CAV was administered in one of three different dosing schedules of (i) once per day, (ii) two times per day, and (iii) three times per day for 10 days to achieve concentration-time profiles (Fig. 3, A to C). We sampled the central compartment at 0, 2, 2.5, 3, 3.5, 5, 7.5, 10, 11.5, 14, 20, 22, and 23.5 hours over a 24-hour interval. The peripheral compartments were sampled on days 0, 2, 4, 6, 8, and 10 for quantification of *Mtb*.

The subsequent HFS-TB studies examined a single CAV dosing scheme, designed to achieve a %T_{MIC} of 100% in an intracellular *Mtb* HFS-TB model of H37Ra for 26 days and a sterilizing effect model of *Mtb* H37Rv at pH 5.8. Central and peripheral compartments were sampled for bacterial burden, as described above and in Results.

WGS of CAV-resistant isolates
DNA was extracted from CAV-resistant isolates using the methods described previously (*47*). Sequencing libraries were prepared using KAPA

Biosystem Hyper kit (KK8504). Six-bases-long unique barcodes were added to each sample by ligating Illumina-compatible adapters and after size selection libraries were amplified using four polymerase chain reaction cycles, followed by cleaning using XP beads. About 9 pM of each library was used for sequencing on HiSeq 2500 PE100 (paired-end 100 base pairs). After sequencing, all the reads were sorted on the basis of the attached barcodes using SAM tools (http://samtools.sourceforge.net/). Raw reads were processed to remove adapter artifacts and to deconvolute the set of reads into their constituent isolates. Reads with no identifiable barcode or with a barcode containing one or more ambiguous base calls were excluded. CLC Genomics Workbench (v9.5.2) was used to perform quality control (read quality, nucleotide content, and sequence redundancy) as well as to align sequencing reads to the reference Mtb genome NC_000962 and to make the variants call for SNV detection.

CAV drug assay

Ceftazidime concentrations in the samples collected from the central compartment of HFS-TB were analyzed by liquid chromatography–tandem mass spectrometry in positive ion mode. Ceftazidime and ceftazidime-D5 (internal standard) were purchased from Toronto Research Chemicals and Sigma, respectively. Calibrator, controls, and internal standard were included in each analytical run for quantitation. Stock solutions of ceftazidime and internal standard were prepared in 80:20 methanol/water at a concentration of 1 mg/ml and stored at −20°C. A seven-point calibration curve was prepared by diluting ceftazidime stock solution in drug-free media (0.25, 1, 5, 10, 25, 50, and 100 μg/ml). Quality control samples were prepared by spiking media with stock standards for two levels of controls of 0.4 and 8 μg/ml. Samples were prepared in 96-well microliter plates by adding 10 μl of calibrator, quality controls, or sample to 190 μl of 0.1% formic acid in water containing internal standard (1 μg/ml) followed by vortex. Chromatographic separation was achieved on an Acquity UPLC HSS T3 analytical column (1.8 μm, 50 × 2.1 mm) (Waters) maintained at 30°C at a flow rate of 0.2 ml/min with a binary gradient with a total run time of 6 min. The observed ion mass/charge ratio (m/z) values of the fragment ions were 547.11→468.11 for ceftazidime and 552.15→468.11 ceftazidime-D5. Sample injection and separation were performed using Acquity UPLC interfaced with a Xevo TQ mass spectrometer (Waters). All data were collected using MassLynx version 4.1 SCN810. The limit of quantitation for this assay was 0.25 μg/ml. The between-day and within-day percentage coefficients of variation were 14 and 21%, respectively.

Pharmacokinetic and pharmacodynamic modeling

Ceftazidime, avibactam, rifampin, pyrazinamide, and isoniazid concentrations were analyzed using ADAPT software, as described previously (29). Pharmacokinetic parameter estimates identified in the models were then used to calculate the AUC_{0-24}, AUC_{0-24}/MIC, peak/MIC, and %T_{MIC} in each HFS-TB. For monotherapy experiments, microbial kill versus exposure was examined using the inhibitory sigmoid E_{max} model.

Monte Carlo experiments

Monte Carlo experiments allow for examination of different drug doses to determine whether they will achieve the exposure targets associated with specific rates of microbial kill in patients. We examined this target attainment in at least 10,000 patients; this number is required to stabilize the tail of the variance. Population pharmacokinetic parameter estimates for CAV, and their covariance, for either children or adults that are shown in table S2 were based on studies published previously (13, 38–40), were entered as domain of input into subroutine PRIOR

of ADAPT software. Both normal and lognormal distributions were examined. We used the option for population simulation without noise. The following doses were examined for children with TB: 50, 100, 150, and 200 mg/kg. The following doses were examined for adults with TB: 2, 4, 6, 8, 12, 14, and 16 g. We used two levels of validation. For the first level, we compared the simulated data to determine whether the pharmacokinetic parameter estimates and variances in the simulated subjects were similar to the data sets entered into the domain of input. For the second level of validation, we examined a separate database, such as the one reported to the FDA, to determine whether the drug concentrations achieved by the standard doses were similar to those we identified in our Monte Carlo experiments.

Each of the doses was examined for the ability to achieve, or exceed, the target CAV exposure %T_{MIC} of either 47 or 63% derived in the HFS-TB studies, at each MIC. We examined each of these for MICs ranging from 2 to 128 mg/liter, based on a twofold dilution. The MIC range was from our results in Fig. 2H. Probability of target attainment (PTA) at each MIC was used to calculate the cumulative proportion of patients [also termed cumulative fractional response (CFR)] who would achieve or exceed the target ceftazidime exposure target %T_{MIC} of either 47 or 63%, on summation over the MIC range based on the formula

$$CFR = \sum_{i=1}^{n} PTA_i * F_i$$

where PTA is at each MIC and F is the proportion of isolates at each MIC (i). For avibactam, the target concentration was 1 mg/liter. The percentage of time that avibactam concentration persisted above 1 mg/liter was set to be equal to the %T_{MIC} for ceftazidime (47 or 63%), assuming that ceftazidime only works when sufficient concentrations of avibactam are achieved. We assumed a ceftazidime/avibactam concentration ratio of 4:1 in all simulations, as in the current commercial preparation.

SUPPLEMENTARY MATERIALS

Supplementary material for this article is available at http://advances.sciencemag.org/cgi/content/full/3/8/e1701102/DC1

fig. S1. Relationship between %T_{MIC} and TTP.
table S1. List of mutations in 12 CAV-resistant Mtb strains.
table S2. Pharmacokinetic parameter input into PRIOR versus parameters achieved in 10,000 simulated patients.

REFERENCES AND NOTES

1. K. Dheda, T. Gumbo, N. R. Gandhi, M. Murray, G. Theron, Z. Udwadia, G. B. Migliori, R. Warren, Global control of tuberculosis: From extensively drug-resistant to untreatable tuberculosis. Lancet Respir. Med. 2, 321–338 (2014).

2. K. Dheda, T. Gumbo, G. Maartens, K. E. Dooley, R. McNerney, M. Murray, J. Furin, E. A. Nardell, L. London, E. Lessem, G. Theron, P. van Helden, S. Niemann, M. Merker, D. Dowdy, A. Van Rie, G. K. Siu, J. G. Pasipanodya, C. Rodrigues, T. G. Clark, F. A. Sirgel, A. Esmail, H. H. Lin, S. R. Atre, H. S. Schaaf, K. C. Chang, C. Lange, P. Nahid, Z. F. Udwadia, C. R. Horsburgh Jr., G. J. Churchyard, D. Menzies, A. C. Hesseling, E. Nuermberger, H. McIlleron, K. P. Fennelly, E. Goemaere, E. Jaramillo, M. Low, C. M. Jara, N. Padayatchi, R. M. Warren, The epidemiology, pathogenesis, transmission, diagnosis, and management of multidrug-resistant, extensively drug-resistant, and incurable tuberculosis. Lancet Respir. Med. 5, 291–360 (2017).

3. K. Dheda, J. D. Limberis, E. Pietersen, J. Phelan, A. Esmail, M. Lesosky, K. P. Fennelly, J. te Riele, B. Mastrapa, E. M. Streicher, T. Dolby, A. M. Abdallah, F. Ben-Rached, J. Simpson, L. Smith, T. Gumbo, P. van Helden, F. A. Sirgel, R. McNerney, G. Theron, A. Pain, T. G. Clark, R. M. Warren, Outcomes, infectiousness, and transmission dynamics of patients with extensively drug-resistant tuberculosis and home-discharged patients with programmatically incurable tuberculosis: A prospective cohort study. Lancet Respir. Med. 5, 269–281 (2017).

4. G. V. Bloemberg, P. M. Keller, D. Stucki, A. Trauner, S. Borrell, T. Latshang, M. Coscolla, T. Rothe, R. Homke, C. Ritter, J. Feldmann, B. Schulthess, S. Gagneux, E. C. Böttger, Acquired resistance to bedaquiline and delamanid in therapy for tuberculosis. N. Engl. J. Med. 373, 1986–1988 (2015).

5. A. S. Pym, A. H. Diacon, S. J. Tang, F. Conradie, M. Danilovits, C. Chuchottaworn, I. Vasilyeva, K. Andries, N. Bakare, T. De Marez, M. Haxaire-Theeuwes, N. Lounis, P. Meyvisch, B. Van Baelen, R. P. van Heeswijk, B. Dannemann; TMC207-C209 Study Group, Bedaquiline in the treatment of multidrug- and extensively drug-resistant tuberculosis. Eur. Respir. J. 47, 564–574 (2016).

6. H. Hoffmann, T. A. Kohl, S. Hofmann-Thiel, M. Merker, P. Beckert, K. Jaton, L. Nedialkova, E. Sahalchyk, T. Rothe, P. M. Keller, S. Niemann, Delamanid and bedaquiline resistance in Mycobacterium tuberculosis ancestral Beijing genotype causing extensively drug-resistant tuberculosis in a tibetan refugee. Am. J. Respir. Crit. Care Med. 193, 337–340 (2016).

7. T. Gumbo, A. J. Lenaerts, D. Hanna, K. Romero, E. Nuermberger, Nonclinical models for antituberculosis drug development: A landscape analysis. J. Infect. Dis. 211 (suppl. 3), S83–S95 (2015).

8. T. Gumbo, J. G. Pasipanodya, K. Romero, D. Hanna, E. Nuermberger, Forecasting accuracy of the hollow fiber model of tuberculosis for clinical therapeutic outcomes. Clin. Infect. Dis. 61 (suppl. 1), S25–S31 (2015).

9. M. Cavaleri, E. Manolis, Hollow fiber system model for tuberculosis: The european medicines agency experience. Clin. Infect. Dis. 61 (suppl. 1), S1–S4 (2015).

10. D. Chilukuri, O. McMaster, K. Bergman, P. Colangelo, K. Snow, J. G. Toerner, The hollow fiber system model in the nonclinical evaluation of antituberculosis drug regimens. Clin. Infect. Dis. 61 (suppl. 1), S32–S33 (2015).

11. S. Ramón-García, R. González del Río, A. S. Villarejo, G. D. Sweet, F. Cunningham, D. Barros, L. Ballell, A. Mendoza-Losana, S. Ferrer-Bazaga, C. J. Thompson, Repurposing clinically approved cephalosporins for tuberculosis therapy. Sci. Rep. 6, 34293 (2016).

12. C. G. Thornton, K. M. MacLellan, T. L. Brink, S. Passen, Characterization of the susceptibility of mycobacteria in BACTEC 12B media containing PANTA that had been supplemented with ceftazidime, and characterization of the individual components of PANTA in the presence of C18-carboxypropylbetaine. J. Microbiol. Methods 56, 243–251 (2004).

13. D. P. Nicolau, L. Siew, J. Armstrong, J. Li, T. Edeki, M. Learoyd, S. Das, Phase 1 study assessing the steady-state concentration of ceftazidime and avibactam in plasma and epithelial lining fluid following two dosing regimens. J. Antimicrob. Chemother. 70, 2862–2869 (2015).

14. G. Kubendiran, C. N. Paramasivan, S. Sulochana, D. A. Mitchison, Moxifloxacin and gatifloxacin in an acid model of persistent Mycobacterium tuberculosis. J. Chemother. 18, 617–623 (2006).

15. A. Jindani, C. J. Doré, D. A. Mitchison, Bactericidal and sterilizing activities of antituberculosis drugs during the first 14 days. Am. J. Respir. Crit. Care Med. 167, 1348–1354 (2003).

16. S. Y. Eum, J. H. Kong, M. S. Hong, Y. J. Lee, J. H. Kim, S. H. Hwang, S. N. Cho, L. E. Via, C. E. Barry III, Neutrophils are the predominant infected phagocytic cells in the airways of patients with active pulmonary TB. Chest 137, 122–128 (2010).

17. W. McDermott, R. Tompsett, Activation of pyrazinamide and nicotinamide in acidic environments in vitro. Am. Rev. Tuberc. 70, 748–754 (1954).

18. T. Gumbo, C. S. W. Dona, C. Meek, R. Leff, Pharmacokinetics-pharmacodynamics of pyrazinamide in a novel in vitro model of tuberculosis for sterilizing effect: A paradigm for faster assessment of new antituberculosis drugs. Antimicrob. Agents Chemother. 53, 3197–3204 (2009).

19. D. Deshpande, S. Srivastava, J. G. Pasipanodya, S. J. Bush, E. Nuermberger, S. Swaminathan, T. Gumbo, Linezolid for infants and toddlers with disseminated tuberculosis: First steps. Clin. Infect. Dis. 63, S80–S87 (2016).

20. D. Deshpande, S. Srivastava, E. Nuermberger, J. G. Pasipanodya, S. Swaminathan, T. Gumbo, Concentration-dependent synergy and antagonism of linezolid and moxifloxacin in the treatment of childhood tuberculosis: The dynamic duo. Clin. Infect. Dis. 63, S88–S94 (2016).

21. Forest Pharmaceuticals, AVYCAZ (Ceftazidime and Avibactam) for Injection, for intravenous use (Reference ID 3949759, Forest Pharmaceuticals, 2016); www.accessdata.fda.gov/drugsatfda_docs/label/2016/206494s002lbl.pdf.

22. T. Gumbo, A. Louie, W. Liu, D. Brown, P. G. Ambrose, S. M. Bhavnani, G. L. Drusano, Isoniazid bactericidal activity and resistance emergence: Integrating pharmacodynamics and pharmacogenomics to predict efficacy in different ethnic populations. Antimicrob. Agents Chemother. 51, 2329–2336 (2007).

23. T. Gumbo, A. Louie, M. R. Deziel, W. Liu, L. M. Parsons, M. Salfinger, G. L. Drusano, Concentration-dependent Mycobacterium tuberculosis killing and prevention of resistance by rifampin. Antimicrob. Agents Chemother. 51, 3781–3788 (2007).

24. M. D. Epstein, N. W. Schluger, A. L. Davidow, S. Bonk, W. N. Rom, B. Hanna, Time to detection of Mycobacterium tuberculosis in sputum culture correlates with outcome in patients receiving treatment for pulmonary tuberculosis. Chest 113, 379–386 (1998).

25. C. Pheiffer, N. M. Carroll, N. Beyers, P. Donald, K. Duncan, P. Uys, P. van Helden, Time to detection of Mycobacterium tuberculosis in BACTEC systems as a viable alternative to colony counting. Int. J. Tuberc. Lung Dis. 12, 792–798 (2008).

26. T. Gumbo, A. Louie, W. Liu, P. G. Ambrose, S. M. Bhavnani, D. Brown, G. L. Drusano, Isoniazid's bactericidal activity ceases because of the emergence of resistance, not depletion of Mycobacterium tuberculosis in the log phase of growth. J. Infect. Dis. 195, 194–201 (2007).

27. T. Gumbo, J. G. Pasipanodya, E. Nuermberger, K. Romero, D. Hanna, Correlations between the hollow fiber model of tuberculosis and therapeutic events in tuberculosis patients: Learn and confirm. Clin. Infect. Dis. 61 (suppl. 1), S18–S24 (2015).

28. T. Gumbo, I. Angulo-Barturen, S. Ferrer-Bazaga, Pharmacokinetic-pharmacodynamic and dose–response relationships of antituberculosis drugs: Recommendations and standards for industry and academia. J. Infect. Dis. 211 (suppl. 3), S96–S106 (2015).

29. D. Deshpande, S. Srivastava, E. Nuermberger, J. G. Pasipanodya, S. Swaminathan, T. Gumbo, A faropenem, linezolid, and moxifloxacin regimen for both drug-susceptible and multidrug-resistant tuberculosis in children: FLAME path on the milky way. Clin. Infect. Dis. 63, S95–S101 (2016).

30. S. Musuka, S. Srivastava, C. W. Siyambalapitiyage Dona, C. Meek, R. Leff, J. Pasipanodya, T. Gumbo, Thioridazine pharmacokinetic-pharmacodynamic parameters "Wobble" during treatment of tuberculosis: A theoretical basis for shorter-duration curative monotherapy with congeners. Antimicrob. Agents Chemother. 57, 5870–5877 (2013).

31. S. Swaminathan, J. G. Pasipanodya, G. Ramachandran, A. K. Hemanth Kumar, S. Srivastava, D. Deshpande, E. Nuermberger, T. Gumbo, Drug concentration thresholds predictive of therapy failure and death in children with tuberculosis: Bread crumb trails in random forests. Clin. Infect. Dis. 63, S63–S74 (2016).

32. J. G. Pasipanodya, H. McIlleron, A. Burger, P. A. Wash, P. Smith, T. Gumbo, Serum drug concentrations predictive of pulmonary tuberculosis outcomes. J. Infect. Dis. 208, 1464–1473 (2013).

33. E. Chigutsa, J. G. Pasipanodya, M. E. Visser, P. D. van Helden, P. J. Smith, F. A. Sirgel, T. Gumbo, H. McIlleron, Impact of nonlinear interactions of pharmacokinetics and MICs on sputum bacillary kill rates as a marker of sterilizing effect in tuberculosis. Antimicrob. Agents Chemother. 59, 38–45 (2015).

34. T. Gumbo, New susceptibility breakpoints for first-line antituberculosis drugs based on antimicrobial pharmacokinetic/pharmacodynamic science and population pharmacokinetic variability. Antimicrob. Agents Chemother. 54, 1484–1491 (2010).

35. T. Gumbo, E. Chigutsa, J. Pasipanodya, M. Visser, P. D. van Helden, F. A. Sirgel, H. McIlleron, The pyrazinamide susceptibility breakpoint above which combination therapy fails. J. Antimicrob. Chemother. 69, 2420–2425 (2014).

36. T. Gumbo, J. G. Pasipanodya, P. Wash, A. Burger, H. McIlleron, Redefining multidrug-resistant tuberculosis based on clinical response to combination therapy. Antimicrob. Agents Chemother. 58, 6111–6115 (2014).

37. X. Zheng, R. Zheng, Y. Hu, J. Werngren, F. L. Davies, M. Mansjö, B. Xu, S. Hoffner, Determination of MIC breakpoints for second-line drugs associated with clinical outcomes in multidrug-resistant tuberculosis treatment in China. Antimicrob. Agents Chemother. 60, 4786–4792 (2016).

38. J. S. Bradley, J. Armstrong, A. Arrieta, R. Bishai, S. Das, S. Delair, T. Edeki, W. C. Holmes, J. Li, K. S. Moffett, D. Mukundan, N. Perez, J. R. Romero, D. Speicher, J. E. Sullivan, D. Zhou, Phase I study assessing the pharmacokinetic profile, safety, and tolerability of a single dose of ceftazidime-avibactam in hospitalized pediatric patients. Antimicrob. Agents Chemother. 60, 6252–6259 (2016).

39. H. Merdjan, M. Rangaraju, A. Tarral, Safety and pharmacokinetics of single and multiple ascending doses of avibactam alone and in combination with ceftazidime in healthy male volunteers: Results of two randomized, placebo-controlled studies. Clin. Drug Investig. 35, 307–317 (2015).

40. D. Hubert, E. Le Roux, T. Lavrut, B. Wallaert, P. Scheid, D. Manach, D. Grenet, I. Sermet-Gaudelus, S. Ramel, C. Cracowski, A. Sardet, N. Wizla, E. Deneuville, R. Garraffo, Continuous versus intermittent infusions of ceftazidime for treating exacerbation of cystic fibrosis. Antimicrob. Agents Chemother. 53, 3650–3656 (2009).

41. A. R. Flores, L. M. Parsons, M. S. Pavelka Jr., Characterization of novel Mycobacterium tuberculosis and Mycobacterium smegmatis mutants hypersusceptible to beta-lactam antibiotics. J. Bacteriol. 187, 1892–1900 (2005).

42. F. Wang, C. Cassidy, J. C. Sacchettini, Crystal structure and activity studies of the Mycobacterium tuberculosis β-lactamase reveal its critical role in resistance to β-lactam antibiotics. Antimicrob. Agents Chemother. 50, 2762–2771 (2006).

43. E. C. Hett, M. C. Chao, E. J. Rubin, Interaction and modulation of two antagonistic cell wall enzymes of mycobacteria. PLOS Pathog. 6, e1001020 (2010).

44. E. C. Hett, M. C. Chao, A. J. Steyn, S. M. Fortune, L. L. Deng, E. J. Rubin, A partner for the resuscitation-promoting factors of Mycobacterium tuberculosis. Mol. Microbiol. 66, 658–668 (2007).

45. C. Modongo, J. G. Pasipanodya, N. M. Zetola, S. M. Williams, G. Sirugo, T. Gumbo, Amikacin concentrations predictive of ototoxicity in multidrug-resistant tuberculosis patients. Antimicrob. Agents Chemother. 59, 6337–6343 (2015).

46. J. A. Seddon, S. Thee, K. Jacobs, A. Ebrahim, A. C. Hesseling, H. S. Schaaf, Hearing
     loss in children treated for multidrug-resistant tuberculosis. *J. Infect.* **66**, 320–329 (2013).
47. S. Srivastava, A. Garg, A. Ayyagari, K. K. Nyati, T. N. Dhole, S. K. Dwivedi, Nucleotide
     polymorphism associated with ethambutol resistance in clinical isolates of
     Mycobacterium tuberculosis. *Curr. Microbiol.* **53**, 401–405 (2006).

Citation: D. Deshpande, S. Srivastava, M. Chapagain, G. Magombedze, K. R. Martin,
K. N. Cirrincione, P. S. Lee, T. Koeuth, K. Dheda, T. Gumbo, Ceftazidime-avibactam has
potent sterilizing activity against highly drug-resistant tuberculosis. *Sci. Adv.* **3**, e1701102
(2017).